Biochemistry

Article

Cite This: Biochemistry 2018, 57, 5507−5512

pubs.acs.org/biochemistry

Open and Closed Form of Maltose Binding Protein in Its Native and Molten Globule State As Studied by Electron Paramagnetic Resonance Spectroscopy

Benjamin Selmke,[†] Peter P. Borbat,[‡] Chen Nickolaus,[†] Raghavan Varadarajan,[§] Jack H. Freed,[‡] and Wolfgang E. Trommer*[,†]

[†]Department of Chemistry, TU Kaiserslautern, Erwin-Schrödinger-Strasse 54, 67663 Kaiserslautern, Germany

[‡]Department of Chemistry and Chemical Biology, ACERT National Biomedical Center for Advanced ESR Technology, Cornell University, Ithaca, New York 14853-1301, United States

[§]Molecular Biophysics Unit, Indian Institute of Science, Bangalore 560012, India

Supporting Information

ABSTRACT: An intensively investigated intermediate state of protein folding is the molten globule (MG) state, which contains secondary but hardly any tertiary structure. In previous work, we have determined the distances between interacting spins within maltose binding protein (MBP) in its native state using continuous wave and double electron−electron resonance (DEER) electron paramagnetic resonance (EPR) spectroscopy. Seven double mutants had been employed to investigate the structure within the two domains of MBP. DEER data nicely corroborated the previously available X-ray data. Even in its MG state, MBP is known to still bind its ligand maltose. We therefore hypothesized that there must be a defined structure around the binding pocket of MBP already in the absence of tertiary structure. Here we have investigated the functional and structural difference between native and MG state in the open and closed form with a new set of MBP mutants. In these, the spin-label positions were placed near the active site. Binding of its ligands leads to a conformational change from open to closed state, where the two domains are more closely together. The complete set of MBP mutants was analyzed at pH 3.2 (MG) and pH 7.4 (native state) using double-quantum coherence EPR. The values were compared with theoretical predictions of distances between the labels in biradicals constructed by molecular modeling from the crystal structures of MBP in open and closed form and were found to be in excellent agreement. Measurements show a defined structure around the binding pocket of MBP in MG, which explains maltose binding. A new and important finding is that in both states ligand-free MBP can be found in open and closed form, while ligand-bound MBP appears only in closed form because of maltose binding.

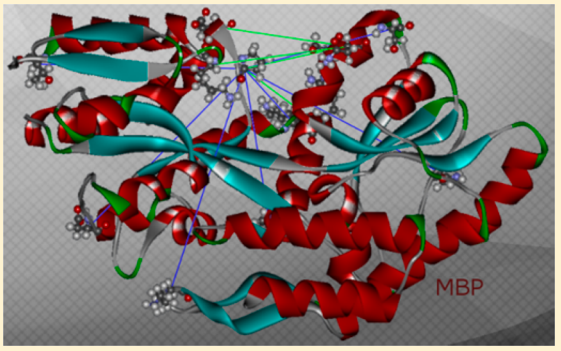

The complex mechanisms of protein folding are still not well understood, although they play an important role in protein function and biological processes.[1] Most models of protein folding introduce so-called "folding pathways", where protein folding is a process of multidimensional routes and intermediate conformations strongly influenced by their environment instead of a single route.[2]

The molten globule (MG) state is an intermediate in this process and is therefore extensively examined as a key in understanding protein folding.[3] It contains a nativelike secondary structure but fluctuating tertiary structures.[4] MG states contain exposed hydrophobic pockets that allow for reaction with the dye 8-anilinonaphthalene-1-sulfonic acid (ANS). Circular dichroism, fluorescence spectroscopy, and nuclear magnetic resonance have been employed to examine the MG.[5]

Relative to the methods mentioned above, electron paramagnetic resonance (EPR) together with site-directed spin labeling yields complementary information about the distance between the spin-labels at selected positions within the biological molecule.[6,7] In combination with molecular dynamics (MD) simulations, measured distances of spin-labels can be related to specific protein models and conformations.[8] The reason to use double-quantum coherence (DQC) EPR is that in most cases a considerably better Tikhonov reconstruction of $P(r)$ could be achieved (see the Supporting Information).[6,9−12] It works very well over a broad range of distances, which includes the short distance range down to ∼1 nm, yielding very good sensitivity.[13−16] Low-background dipolar traces in DQC simplify the reconstruction by the typically used L-curve regularization method.[11,17]

Received: March 16, 2018
Revised: July 12, 2018
Published: July 13, 2018

DOI: 10.1021/acs.biochem.8b00322
Biochemistry 2018, 57, 5507−5512

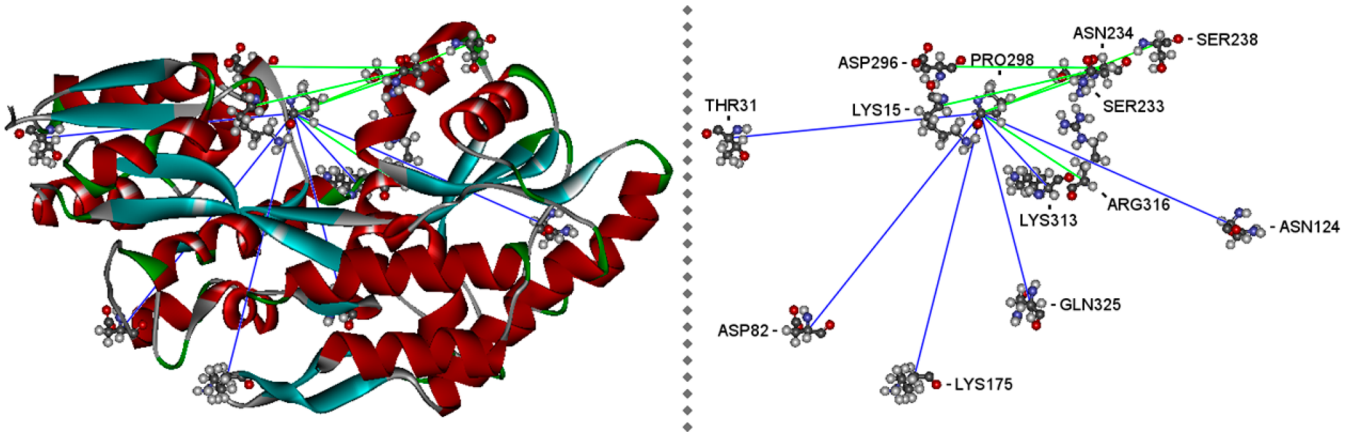

Figure 1. Overview of the complete set of MBP mutants in open state MBP (Protein Data Bank entry 1OMP). Blue lines indicate Cα amino acid distances of mutants MBP 01−06. Green lines indicate Cα amino acid distances of mutants MBP 07−11.

Maltose binding protein (MBP) is a 370-amino acid, periplasmic protein of *Escherichia coli* involved in chemotaxis for the uptake of a range of maltose sugars. MBP is a single-chain monomeric two-domain protein devoid of any cofactors.[18] Binding of its ligands leads to a conformational change from open (Figure 1) to closed state, where the two domains are more closely together. It has been employed extensively to monitor folding dynamics and to determine the corresponding thermodynamic parameters. Unlike other large proteins, MBP undergoes reversible unfolding and the MG state can be stabilized at pH 3.2.[4] ITC measurements show that even in its MG state MBP can still bind its ligand, maltose.[19,20]

MATERIALS AND METHODS

Materials. All reagents were from commercial sources and of analytical grade. (1-Oxyl-2,2,5,5-tetramethyl-pyrroline-3-methyl)-methanethiosulfonate (MTS) was a kind gift from K. Hideg (University of Pécs, Pécs, Hungary).

Mutants and Plasmids. The plasmids of double mutants MBP 09 (P298C_R316C), 10 (N234C_D296C), and 11 (N234C_K015C) were constructed by site-directed mutagenesis employing standard techniques.[21] Mutants MBP 01 (P298C_T031C), 02 (P298C_D082C), 03 (P298C_N124C), 04 (P298C_K175C), 05 (P298C_K313C), 06 (P298C_Q325C), and 07 (P298C_S238C) are described in ref 22. An overview of the complete set of mutants and their positions is given in Figure 1.

The complete MBP sequences of all mutants were determined by Sanger sequencing at Seq-it, Kaiserslautern, Germany.

Protein Purification, Spin Labeling, and Sample Preparation. Wild type (WT) (UniProtKB entry P0AEX9) and mutant proteins were expressed in *E. coli* strain DH5α.[4] Cells were grown in TB medium containing 100 μg/mL ampicillin at 37 °C. The culture was induced with 2 mM isopropyl β-D-thiogalactopyranoside (IPTG) at an OD_{600} of 2. After being incubated for 12 h, cells were pelleted at 6000 rpm and 4 °C and washed by being resuspended in 20 mM Tris-NaCl buffer (pH 7.4). Cell lysis was achieved through processing in a French press. The lysate was subjected to centrifugation at 13000 rpm and 4 °C before the proteins were extracted by affinity chromatography on an amylose column at 4 °C.[23]

To remove maltose, MBP was dialyzed at room temperature in Tris-NaCl buffer containing 6 M urea to completely release maltose from MBP. MBP was slowly refolded by drop dilution in Tris-NaCl buffer and concentrated on a Q-Sepharose column. The protein concentration was estimated by the method of Lowry with bicinchoninic acid (BCA), and the purity of the proteins was assayed by sodium dodecyl sulfate−polyacrylamide gel electrophoresis and matrix-assisted laser desorption ionization time-of-flight mass spectrometry. The removal of maltose was proven by a coupled maltose assay (Sigma-Aldrich) in which maltose was degraded to glucose (α-glucosidase) and further phosphorylated (hexokinase) and dehydrogenated (glucose-6-phosphate dehydrogenase) to 6-phosphogluconate.[20]

Spin labeling was performed as described in ref 22 with the exception that desalting and buffer exchange were achieved through dialysis (under dark conditions) instead of a PD-10 column and a 3-fold molar excess of MTS was used. The protein samples for MG measurements were slowly adjusted to pH 3.2 during dialyses (under dark conditions).

The EPR samples were prepared in CGH5 (citrate, glycine, and HEPES, 5 mM each) buffer with 50−100 μM protein, 20% (v/v) glycerol, and 20 mM maltose if required.

All of the samples were shock frozen and stored at −80 °C until they were used.

EPR Experiment. The DQC and DEER experiments were performed at ACERT, Ithaca, New York, USA.

Pulse dipolar EPR spectroscopy (PDS) experiments on MBP samples were performed at 60 K and a 17.3 GHz frequency using a home-built Ku-band PDS spectrometer at ACERT.[24,25] All MBP samples were measured by DQC using the six-pulse sequence $\pi/2-t_p-\pi-t_p-\pi/2-t_d-\pi-t_d-\pi/2-(t_m-t_p)-\pi-(t_m-t_p)-$echo for all conditions.[10,11] In addition, DEER measurements were taken on selected samples, which all had distances well in the "DEER range" for all four conditions used.[26,27] DQC in most cases used $\pi/2$ and π pulses of 3 and 6 ns, respectively, and the sequence was applied at the center of the spectrum. DEER used 16 and 32 ns pulses for detection and a 16 ns pump pulse. The setup for DEER was standard with the detection sequences applied at the low-field edge of the spectrum.[28]

Examples of DQC and (some) DEER data are included in the Supporting Information. The rest of the data that is not shown was of the same quality. The data were collected usually in 1−4 h, but ∼12 h was used in several cases to yield high

DOI: 10.1021/acs.biochem.8b00322
Biochemistry 2018, 57, 5507−5512

SNR. The time-domain DEER data were always in very good agreement with the respective DQC data, and the distance distributions, $P(r)$'s, were thus close to that obtained from DQC, agreeing well, for example, in the bimodal characters and other details. This also indicated that these details were unlikely to originate from (usually weak) orientation effects.

The L-curve Tikhonov regularization followed by the refinement with the maximum-entropy method was used for distance reconstruction.[17,29] Because the DQC data had only a very small background, the backgrounds were approximated accurately by a linear function and subtracted out. The stability of distance reconstruction was high in DQC, and the results have shown only a very minor contribution of spurious peaks, which is characteristic for DQC and is clear from the examples in the Supporting Information.

MD Simulation. For the MD simulation of MBP, the software Accelrys Discovery Studio 2.5.5 and the X-ray structures 1ANF and 1OMP from the RCSB Protein Data Bank were used.[30] The structures were typed by the CHARMm force field and minimized. For all simulations, the implicit water model generalized Born with a simple switching (dielectric constant of 1, implicit solvent dielectric constant of 80, nonpolar surface area of true, salt concentration of 0, van der Waals radii, and molecular surface of true), a dynamic integrator of Leapfrog Verlet, a nonbond list radius of 14, spherical cutoff electrostatics, and no SHAKE constraint were used. For energy minimization, a minimization cascade of steepest descent followed by conjugated gradient and adopted basis Newton−Raphson algorithm was used. For the simulation of 1OMP, the ligand maltose was removed. Water molecules were removed from both structures.

All mutants were simulated through mutation of the pair of respective cysteines, addition of MTS fragments to the sulfide groups, and retyping by the CHARMm force field. To find an appropriate starting position for dynamic simulation, the complete system was at first minimized with fixed constraints over the complete protein area, including the ligand without cysteines and MTS. The minimization was continued using harmonic restraints with a force constant of 8 over the same area and again using harmonic restraints with a force constant of 4 over all hydrophobic amino acids, including the ligand without cysteines (Hydrophob-Cys). Then an explicit water environment was placed around the MTS binding site using explicit spherical boundary with harmonic restraint with a sphere radius of 1.5 nm to obtain a realistic environment for the spin-label.[31] For the dynamic simulation of the complete system, harmonic restraints with a force constant of 0.2 for all water molecules and the restraints Hydrophob-Cys were used.

The MTS distance area was determined in the 40 ps production step of a dynamic cascade simulation (minimization, heating and cooling, equilibration, production).

RESULTS AND DISCUSSION

The Open and Closed Form Can Be Detected for Ligand-Free MBP. The EPR measurements show in most cases more rotamers of MBP and a different proportion of distances in the ligand-free MBP than in the MBP samples with an excess of maltose.

The MTS distances in open and closed state MBP are calculated through MD simulation and fit very well in comparison to DQC data. Because of this comparison, these rotamers can be assigned to open and closed state MBP. The loss of signal for the rotamers assigned to open state MBP in maltose-bound DQC measurements confirms these assignments (Figure 3).

As an example, the distance distribution of MBP 07 at pH 7 without maltose is shown in Figure 2 and the rotamers of closed and open state MBP are marked. The measurement of the same sample with maltose only shows the MTS distances of the rotamers of closed state MBP in native and MG, as shown in Figure 3g and the Supporting Information.

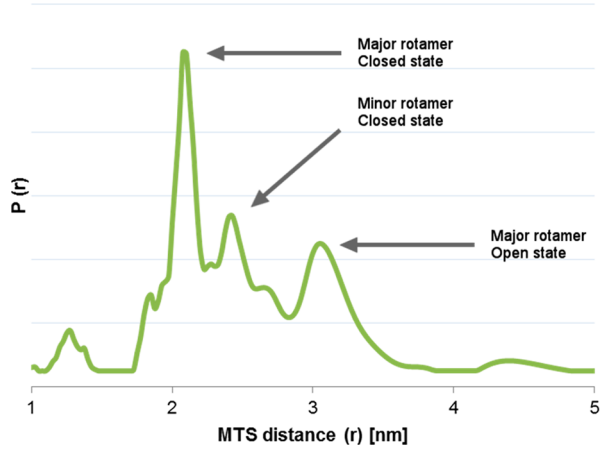

Figure 2. Distance distribution of MTS distances for MBP 07 (P298C_S238C) at pH 7 without maltose. Rotamers of closed and open state MBP are marked.

The comparison between simulated distances and DQC data for open and closed state MBP for all mutants is shown in Table 1. DQC distance distributions can be seen in Figure 3.

For mutants MBP 09 and 10, the closed state could not be measured because of the <1 nm distance. In the case of MBP 04 at pH 7 with maltose, no DQC distance could be obtained, and because of the already high level of agreement of spectra between maltose-bound native and MG structure, the measurement was not repeated.

Table 1 shows the high level of agreement of MD simulated data and DQC measurements for all mutants. Mutants MBP 01−07 represent distances covering a broad range of the structure of the complete protein as described in ref 22. Mutants 09−11 provide further insight into the structure near the active binding site. In combination, good insight about the overall protein conformation is obtained.

The Supporting Information provides typical examples and their detailed interpretation of the DQC spectra for mutants 01 (Figure S5), 07 (Figure S6), and 09 (Figure S7).

In most cases, the distances in open state MBP are larger than in closed state MBP, but as shown in simulated data and the accompanying loss of signal with excess of maltose, mutants MBP 04 and MBP 02 are exceptions. In those, the MTS distance in the closed state is larger than in the open state, which can be seen in the MD simulation (Table 1) and explained by the cysteine position and adjustment of the spin-label. The measurements of MBP 02 show only a small difference, while MBP 04 presents a large difference of ∼1 nm in the MTS distance between both states.

For ligand-bound mutant MBP 02, the major closed state rotamer can be found at 3.4 nm in addition to a minor rotamer at 4.1 nm, which is not seen in the absence of maltose, when the open form dominates. As open and closed forms overlap at 3.3 and 3.6 nm, individual rotamers are not clearly visible.

DOI: 10.1021/acs.biochem.8b00322
Biochemistry 2018, 57, 5507−5512

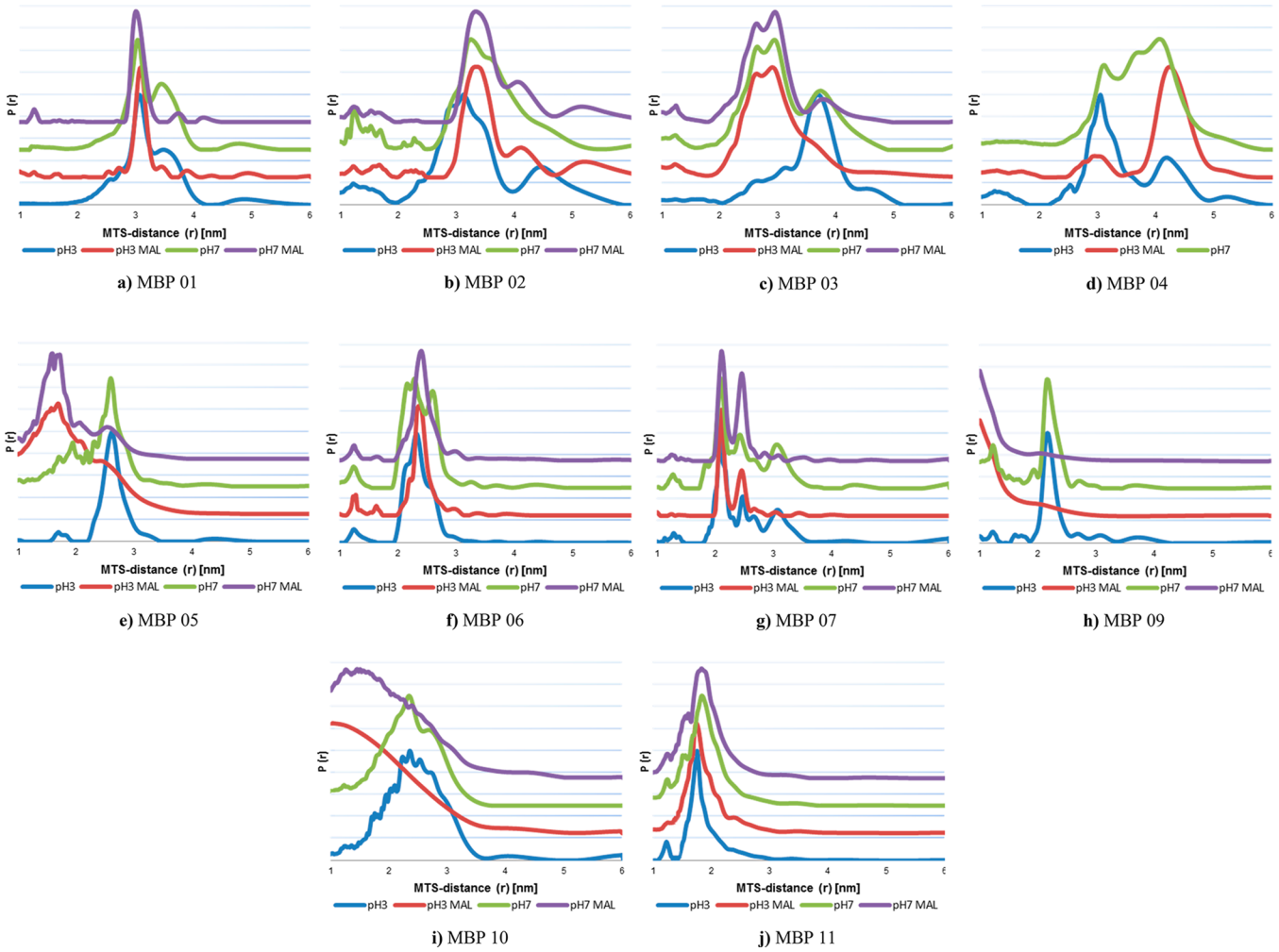

Figure 3. Distance distribution of MTS distances in mutants MBP 01−11 in the native (pH 7) and MG (pH 3.2) states with and without maltose. More rotamers can be seen in measurements without maltose (blue and green), indicating open state distances.

Mutant MBP 03 exhibits a higher proportion of rotamers in the open state, both at pH 7 and at pH 3, as compared to spectra in the presence of maltose. Mutant MBP 05 shows a relatively broad distribution of rotamers in the closed state indicating a higher mobility of the labels as well as of the protein backbone in this region. This can be seen especially well in the broader distribution of pH 3 Mal as compared to that of pH 7 Mal. The difference between open and closed forms of MBP is best seen in Figure 3e.

Hence, the measurements allow for detection of the open and closed conformations of MBP. Even without a ligand, MBP is found in the open and closed conformations.

Even in the MG State, the Structure of MBP Resembles the Structure of the Native State. As shown by ANS binding and CD measurements, MBP is in a stabilized MG state at pH 3.2.[19] We verified that all MBP double mutants also show the loss of tertiary structure as demonstrated by ANS binding measurements at pH 3.2 as shown for example in ref 22.

DQC measurements compared between the native and MG state only show a small broadening of peaks in the case of pH 3.2 as one can see in Figure 3. All rotamers of open and closed state MBP can be found in native and MG measurements, so the simulated MTS distances in Table 1 can be applied to determine the open and closed states of MBP in the MG state. Earlier findings of DEER measurements for MBP 03 at pH 3.3 published in ref 22 pointing to individual helices pointing in all possible directions for MBP in MG can now be newly interpreted. Those earlier data showed two broad peaks at 2.67 and 3.85 nm that can be now connected to open and closed state MBP through loss of maltose through sample preparation and pH adjustment, exactly explaining the newly formed peak in the pH 3.3 measurement.

In the measurements of label positions farther from the maltose binding pocket (MBP 01−06) a stronger tendency to the open state in case of ligand-free MBP can be seen for the MG state. In the presence of an excess of maltose, only the closed state of MBP can be detected even in the MG state. In the vicinity of the active site (MBP 07−11), the structures hardly differ between the MG and native state as shown by EPR spectroscopy. These findings corroborate previous findings that MBP can still bind maltose in the MG state and confirm the assumption that a defined structure of MBP exists near the binding pocket even in the MG state.[4,33]

CONCLUSION

In combination with MD simulation, analysis of MTS distances in mutants MBP 01−11 reveals the changes between open and closed state and ligand binding. Even in the absence of its ligand, MBP can be found in the open and closed states. This

DOI: 10.1021/acs.biochem.8b00322
Biochemistry 2018, 57, 5507−5512

Table 1. Comparison between Simulated Spin-Label Distances and DQC Data for Open and Closed State MBP[a]

			DQC MTS distance (nm)	
mutant	state	simulated MTS distance (nm)	peak	rmsd
MBP 01	open	3.5−3.6	3.6	0.3
	closed	3.1−3.2	3	0.2
MBP 02	open	3.3−3.5	3.3 and 3.5	0.3 and 0.3
	closed	3.4−3.6	3.4	0.2
MBP 03	open	3.5−3.6	3.7	0.3
	closed	2.6−2.8	2.6 and 3.0	0.2 and 0.2
MBP 04	open	3.0−3.1	3.1	0.2
	closed	4.1−4.3	3.6 and 4.0	0.2 and 0.2
MBP 05	open	2.5−2.6	2.6	0.2
	closed	1.7−1.8	1.6 and 1.7	0.1 and 0.1
MBP 06	open	2.6−2.7	2.3 and 2.6	0.2 and 0.1
	closed	2.3−2.4	2.4	0.1
MBP 07	open	2.6−2.8	3	0.2
	closed	2.0−2.2	2.1 and 2.4	0.1 and 0.1
MBP 09	open	1.9−2.1	2.2	0.1
	closed	0.9−1.1	X	X
MBP 10	open	2.2−2.4	2.3	0.5
	closed	0.5−0.7	X	X
MBP 11	open	1.1−1.3	1.2	0.1
	closed	1.7−1.8	1.8	0.3

[a]Specifically, the distance between the nitroxide groups of MTS. The simulated distances fit very well for measured DQC data.

corroborates previous findings of Reif and co-workers that MalF interacts with MBP in a manner independent of maltose.[32] Through DQC measurements, it was proven that MBP keeps a nativelike structure, especially around the binding pocket, in the MG state, thus explaining the ability of MBP to bind its ligands in the MG state. Open and closed forms of MBP exist in the absence of maltose, both in the native and in the MG form.

■ ASSOCIATED CONTENT

Supporting Information

The Supporting Information is available free of charge on the ACS Publications website at DOI: 10.1021/acs.biochem.8b00322.

Illustration of PDS data, mostly DQC and some DEER, used in this work (Figures S1−S3) and exemplary DQC data and according distance distributions (Figures S4−S7) (PDF)

■ AUTHOR INFORMATION

Corresponding Author

*Department of Chemistry, TU Kaiserslautern, P.O. Box 3049, D-67663 Kaiserslautern, Germany. Phone: +49-631-205 2045. Fax: +49-631-205 3419. E-mail: trommer@chemie.uni-kl.de.

ORCID

Raghavan Varadarajan: 0000-0002-2693-5248
Jack H. Freed: 0000-0003-4288-2585
Wolfgang E. Trommer: 0000-0002-2092-2227

Notes

The authors declare no competing financial interest.

■ ACKNOWLEDGMENTS

This work was supported in part by NIH grant P41GM103521.

■ ABBREVIATIONS

ANS, 8-anilinonaphthalene-1-sulfonic acid; CW, continuous wave; DEER, double electron−electron resonance; DQC, double-quantum coherence; EPR, electron paramagnetic resonance; ITC, isothermal titration calorimetry; MBP, maltose binding protein; MD, molecular dynamics; MG, molten globule; MTS, (1-oxyl-2,2,5,5-tetramethyl-pyrroline-3-methyl)-methanethiosulfonate.

■ REFERENCES

(1) Alberts, B., Johnson, A., Lewis, J., Morgan, D., Raff, M., Roberts, K., and Walter, P. (2002) *Molecular Biology of the Cell*, 4th ed., Garland Science, New York.

(2) Wolynes, P., Onuchic, J., and Thirumalai, D. (1995) Navigating the folding routes. *Science 267*, 1619−1620.

(3) Kuwajima, K. (1989) The molten globule state as a clue for understanding the folding and cooperativity of globular-protein structure,. *Proteins: Struct., Funct., Genet. 6* (2), 87−103.

(4) Prajapati, R. S., Indu, S., and Varadarajan, R. (2007) Identification and Thermodynamic Characterization of Molten Globule States of Periplasmic Binding Proteins. *Biochemistry 46*, 10339−10352.

(5) Ohgushi, M., and Wada, A. (1983) 'Molten-globule state': a compact form of globular proteins with mobile side-chains. *FEBS Lett. 164* (1), 21−24.

(6) Borbat, P. P., and Freed, J. H. (1999) Multiple-quantum ESR and distance measurements. *Chem. Phys. Lett. 313*, 145−154.

(7) Jeschke, G., and Polyhach, Y. (2007) Distance measurements on spin-labelled biomacromolecules by pulsed electron paramagnetic resonance. *Phys. Chem. Chem. Phys. 9*, 1895−1910.

(8) Steinhoff, H. J., Radzwill, N., Thevis, W., Lenz, V., Brandenburg, D., Antson, A., Dodson, G., and Wollmer, A. (1997) Determination of Interspin Distances between Spin-Labels Attached to Insulin: Comparison of EPR Data with the X-ray analysis Structure. *Biophys. J. 73*, 3287−3298.

(9) Borbat, P. P., Costa-Filho, A. J., Earle, K. A., Moscicki, J., and Freed, J. H. (2001) Electron spin resonance in studies of membranes and proteins. *Science 291* (5502), 266−269.

(10) Borbat, P. P., McHaourab, H. S., and Freed, J. H. (2002) Protein structure determination using long-distance constraints from double-quantum coherence ESR: Study of T4 Lysozyme. *J. Am. Chem. Soc. 124*, 5304−5314.

(11) Borbat, P. P., and Freed, J. H. (2017) Dipolar Spectroscopy - Single-resonance Methods. *Emagres 6* (4), 465−493.

(12) Borbat, P. P., and Freed, J. H. (2013) *Pulse Dipolar Electron Spin Resonance: Distance Measurements*, Springer-Verlag, Berlin.

(13) Gaffney, B. J., Bradshaw, M. D., Frausto, S., Wu, F., Freed, J. H., and Borbat, P. P. (2012) Locating a Lipid at the Portal to the Lipoxygenase Active Site. *Biophys. J. 103* (10), 2134−2144.

(14) Merz, G. E., Borbat, P. P., Pratt, A. J., Getzoff, E. D., Freed, J. H., and Crane, B. R. (2014) Copper-Based Pulsed Dipolar ESR Spectroscopy as a Probe of Protein Conformation Linked to Disease States. *Biophys. J. 107* (7), 1669−1674.

(15) Fafarman, A. T., Borbat, P. P., Freed, J. H., and Kirshenbaum, K. (2007) Characterizing the structure and dynamics of folded oligomers: Pulsed ESR studies of peptoid helices. *Chem. Commun.* No. 4, 377−379.

(16) Orlando, B. J., Borbat, P. P., Georgieva, E. R., Freed, J. H., and Malkowski, M. G. (2015) Pulsed Dipolar Spectroscopy Reveals That Tyrosyl Radicals Are Generated in Both Monomers of the Cyclooxygenase-2 Dimer. *Biochemistry 54* (50), 7309−7312.

DOI: 10.1021/acs.biochem.8b00322
Biochemistry 2018, 57, 5507−5512

(17) Chiang, Y. W., Borbat, P. P., and Freed, J. H. (2005) The determination of pair distance distributions by pulsed ESR using Tikhonov regularization. *J. Magn. Reson. 172* (2), 279−295.
(18) Spurlino, J. C., Quiocho, F. A., and Lu, G. Y. (1991) The 2.3-Å resolution structure of the maltose- or maltodextrin- binding protein, a primary receptor of bacterial active transport and chemotaxis. *J. Biol. Chem. 266* (8), 5202−5219.
(19) Sheshadri, S., Lingaraju, G. M., and Varadarajan, R. (1999) Denaturant mediated unfolding of both native and molten globule states of maltose binding protein are accompanied by large ΔCṕs. *Protein Sci. 8*, 1689−1695.
(20) Nickolaus, C. (2017) The Molten Globule State of Maltose-Binding Protein: Structural Characterization by Electron Paramagnetic Resonance Spectroscopy. Ph.D. Dissertation, TU Kaiserslautern, Kaiserslautern, Germany.
(21) *QuikChange II XL Site-Directed Mutagenesis Kit: Instruction Manual*, revision 064001c (2004) Stratagene.
(22) Reichenwallner, J., Chakour, M., Indu, S., Varadarajan, R., and Trommer, W. E. (2013) Maltose Binding Protein Is Partially Structured in Its Molten Globule State. *Appl. Magn. Reson. 44* (8), 983−995.
(23) *pMALTM Protein Fusion and Purification System, Instruction Manual*, manual E8200 (2007) New England Biolabs Inc.
(24) Borbat, P. P., Crepeau, R. H., and Freed, J. H. (1997) Multifrequency two-dimensional Fourier transform ESR: an X/Ku-band spectrometer. *J. Magn. Reson. 127* (2), 155−167.
(25) Borbat, P. P., Georgieva, E. R., and Freed, J. H. (2013) Improved Sensitivity for Long-Distance Measurements in Biomolecules: Five-Pulse Double Electron-Electron Resonance. *J. Phys. Chem. Lett. 4* (1), 170−175.
(26) Banham, J. E., Baker, C. M., Ceola, S., Day, I. J., Grant, G. H., Groenen, E. J. J., Rodgers, C. T., Jeschke, G., and Timmel, C. R. (2008) Distance measurements in the borderline region of applicability of CW EPR and DEER: A model study on a homologous series of spin-labelled peptides. *J. Magn. Reson. 191* (2), 202−218.
(27) Borbat, P. P., and Freed, J. H. (2007) Measuring distances by pulsed dipolar ESR spectroscopy: Spin-labeled histidine kinases. In *Two-Component Signaling Systems. Part B* (Simon, M. I., Crane, B. R., and Crane, A., Eds.) Vol. *423*, pp 52−116, Elsevier Academic Press Inc., San Diego.
(28) Georgieva, E. R., Borbat, P. P., Norman, H. D., and Freed, J. H. (2015) Mechanism of influenza A M2 transmembrane domain assembly in lipid membranes. *Sci. Rep. 5*, 11757.
(29) Chiang, Y. W., Borbat, P. P., and Freed, J. H. (2005) Maximum entropy: A complement to Tikhonov regularization for determination of pair distance distributions by pulsed ESR. *J. Magn. Reson. 177* (2), 184−196.
(30) Quiocho, F. A., Spurlino, J. C., and Rodseth, L. E. (1997) Extensive features of tight oligosaccharide binding revealed in high-resolution structures of the maltodextrin transport/chemosensory receptor. *Structure 5* (8), 997−1015.
(31) White, R. P., and Meirovitch, H. (2006) Minimalist explicit solvation models for surface loops in proteins. *J. Chem. Theory Comput. 2* (4), 1135−1151.
(32) Jacso, T., Grote, M., Daus, M. L., Schmieder, P., Keller, S., Schneider, E., and Reif, B. (2009) Periplasmic Loop P2 of the MalF Subunit of the Maltose ATP Binding Cassette Transporter Is Sufficient To Bind the Maltose Binding Protein MalE. *Biochemistry 48*, 2216−2225.
(33) Selmke, B., Chen, N., Borbat, P., Freed, J. H., and Trommer, W. E. (2017) The molten globule state of maltose binding protein: structural characterization by EPR spectroscopy. *Biophys. J. 112*, 485A−486A.

■ NOTE ADDED AFTER ASAP PUBLICATION

This paper was published ASAP on September 13, 2018, with errors in some of the reference citations. The corrected version was reposted on September 13, 2018.

DOI: 10.1021/acs.biochem.8b00322
Biochemistry 2018, 57, 5507−5512